

SPECT/CT scatter estimation using a deep convolutional neural network: implementation in Y-90 imaging

Haowei Xiang, *Student Member, IEEE*, Hongki Lim, *Student Member, IEEE*,
Jeffrey A. Fessler, *Fellow, IEEE*, and Yuni K. Dewaraja, *Member, IEEE*

Abstract—Monte Carlo (MC) based scatter modeling in Y-90 bremsstrahlung SPECT has demonstrated improved image quality and quantitative accuracy, but at the expense of computational complexity. We present a deep learning approach for SPECT/CT scatter estimation that substantially reduces the computation time. Once trained, our deep Convolutional Neural Network (CNN) takes the projections from the SPECT camera and CT-based attenuation map as input and outputs the scatter projections. MC simulated digital phantom data, where true scatter is known, is used during the training process and the network is trained to match the MC scatter estimation. For our network, Adam is used as optimizer, the learning rate is $1e-4$, the mean square error is used as loss, the batch size is 32, and we train this CNN with 100 epochs. In testing with a hot sphere phantom simulation and a liver phantom measurement, visual image quality and contrast recovery was similar with the CNN and MC scatter estimation methods, but the CNN scatter estimate was generated in a fraction of the time needed for the MC scatter estimation (about 1 min for CNN vs 1-2 hours for MC). The short processing time with CNN while maintaining accuracy has high clinical significance for quantitative Y-90 SPECT imaging.

I. INTRODUCTION

ACCURATE scatter estimation is essential for quantitative SPECT applications. It is generally accepted that the Monte Carlo (MC) method that fully models the physics of photon transport in the patient and camera provides the most accurate scatter estimation. However, since MC simulation is very computationally expensive, simpler but less accurate methods such as energy window based estimates are commonly used in clinics. However, energy window based methods are generally valid only for gamma-ray emitters with associated photopeak(s) and not for bremsstrahlung photons where the energy spectrum is continuous. MC based scatter modeling in Y-90 bremsstrahlung SPECT imaging has demonstrated improved image quality and quantitative accuracy [1][2].

We propose a deep learning based scatter estimation that has the potential to overcome the accuracy - computation efficiency trade-off of MC and energy-window based methods. While our proposed method can be generalized to any SPECT

imaging study, we implement and evaluate it here for the challenging case of scatter compensation in Y-90 bremsstrahlung SPECT/CT. The Y-90 bremsstrahlung photon energies extend up to 2.3 MeV, and there is substantial downscatter of the higher energy photons into the lower energy acquisition windows that are typically set in the range 100 - 250 keV. We compare the performance of our proposed method with results from our previous Monte Carlo scatter model [1] as well as the true scatter (available in the case of simulated data) in clinically relevant phantom simulations and measurements.

Recently, deep learning methods have been proposed for fast scatter estimation in PET [3][4] and CT [5] reconstruction. For SPECT scatter correction, although artificial neural networks trained on spectral analysis were proposed over 2 decades ago [6][7], to our knowledge, there have been no studies that exploit the recent advances in deep learning.

II. METHODS

Our deep Convolutional Neural Network (CNN) takes the projections from the SPECT camera and the projected CT-based attenuation map as input and outputs the scatter estimation for each projection. We use MC [8] simulated true scatter as reference and the CNN is trained to minimize the mean square error (MSE) between the output and the reference. The MC (SIMIND) simulation model includes full photon transport in the patient and SPECT camera, including scatter effects in the patient, collimator, detector, and backscatter. MC simulation is only needed during the training process since the network is trained to match the SIMIND scatter estimation.

A. Reconstruction model

Ordered Subset Expectation Maximization (OSEM) is used for image reconstruction. The generated scatter estimate, s , is included as an additive term in the forward model: $y = Ax + s$, where A is the system matrix, y is the measured projections, and x is the unknown image. All of our results use 30 OSEM iteration with eight subsets, which is sufficient to let the metrics converge based on our observation.

B. Simulated data generation

A challenge with using deep learning in SPECT scatter correction is the fact that the ground truth (true scatter) is unknown in measurements. To obtain enough data with known ground

Manuscript received December 14, 2019. This work was supported by NIH-NIBIB grant R01EB022075.

H. Xiang, H. Lim, and J. A. Fessler are with the Department of Electrical Engineering and Computer Science, University of Michigan, Ann Arbor, MI 48109, USA (e-mail: haoweix@umich.edu).

Y. K. Dewaraja is the Department of Radiology, University of Michigan, Ann Arbor, MI 48109, USA.

truth for training/testing, SPECT projections, typically 128, corresponding to different digital phantoms were generated by SIMIND. These digital phantoms were 1) NEMA-like PET phantom with sphere volumes expanded to be more relevant to SPECT 2) a hot sphere Data Spectrum phantom and 3) six virtual patient phantoms that we generated from SPECT and segmented CT images corresponding to six patients who underwent Y-90 SPECT/CT imaging after Y-90 microsphere radioembolization at our clinic. A Symbia Invevo SPECT/CT with high energy collimators and a 105 to 195 keV window was modeled. After each SPECT simulation, the output projections were scaled to a clinically realistic count level before adding Poisson noise.

C. Measured data

Y-90 SPECT/CT measurements from our Symbia Invevo scanner were included in the testing data set. This included a measurement with a physical liver phantom with clinically relevant Y-90 activity levels in the liver and lesion inserts. In the case of measured data, the true scatter is unknown, but the comparison can be made to results from our previous Monte Carlo based scatter estimation method.

D. Network architecture and training procedure

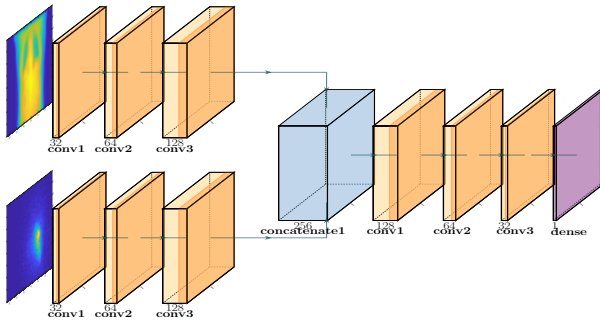


Fig. 1. CNN Diagram: Upper-left input is projection of attenuation map, lower-left is SPECT projection and output is estimated scatter projection.

Figure 1 shows our CNN structure which uses both the SPECT projections and also projection of CT-based attenuation map to estimate scatter. For our CNN, Adam is used as optimizer, the learning rate is $1e-4$, the mean square error is used as loss, the batch size is 32, and we train this CNN with 100 epochs.

The digital Data Spectrum phantom and three virtual patients (512 projections and mumaps in total) are used to train the CNN, and two virtual patients are used for validation.

E. Metrics definition

Activity Recovery (AR) for object i

$$AR = A_i / A_i^{\text{true}} * 100\%, \quad (1)$$

where A_i is the estimated activity, A_i^{true} is the true activity in lesion i .

Contrast Recovery (CR) is defined as

$$CR = \frac{C_i / C_{bkg} - 1}{A_i^{\text{true}} / A_{bkg}^{\text{true}} - 1} * 100\%, \quad (2)$$

where C_i is the mean count in lesion i , C_{bkg} is the mean count in the background, A_{bkg}^{true} is the true activity in the background.

Cold region Residual Error is calculated as

$$Q_i = \frac{C_i}{C_{bkg}} * 100\%, \quad (3)$$

with the same notation as before.

III. RESULTS

A. Training Process

Figure 2 shows the Mean Square Error (MSE) vs. epochs for training and validation.

It takes about 8 hours to train this CNN on an i5 CPU and approximately half an hour to train on a GTX 1080 8GB GPU.

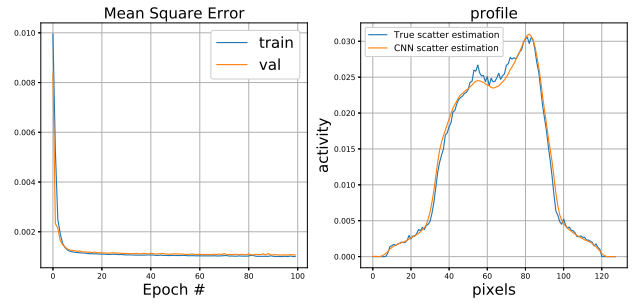


Fig. 2. Training and validation MSE (left) and sample profile in projection domain (right)

B. Phantom test results

The digital NEMA-like phantom and the physical liver phantom were used for testing. For the NEMA-like phantom, a profile across a scatter projection estimated by the CNN is compared with the true scatter from SIMIND in Figure 2. Reconstructed images in Figures 3 and 5 for the digital phantoms and phantom measurement show similar image quality with CNN and MC scatter estimates. Table III-B compares the Contrast Recovery for hot inserts and residual error of the cold lung region in the reconstructed image of the phantoms. Green numbers represent the results using the true scatter estimate, which is regarded as the ground truth (only available for digital phantom). For the NEMA-like phantom, plots of sphere CR vs. iteration in fig 4 also show that results from the proposed method are similar to the MC based results at all iterations.

With our trained CNN it took only about 1 min to generate all 128 scatter projections for each test case. The time to generate the corresponding scatter projections with our previous MC based approach was about 1 hour.

TABLE I
CONTRAST RECOVERY VS. RADIUS: NEMA-LIKE PHANTOM SIMULATION (UPPER) AND LIVER PHANTOM MEASUREMENT (LOWER)

NEMA phantom insert radius (mm)	29	19	16	12	10	8	Lung (cold) residual error
CR (no SC)	0.34	0.30	0.26	0.22	0.21	0.15	0.56
CR (true SC)	0.85	0.80	0.73	0.64	0.67	0.48	0.80
CR (MC [1] SC)	0.77	0.70	0.64	0.59	0.63	0.42	0.61
CR (CNN SC)	0.72	0.73	0.68	0.63	0.65	0.46	0.64

Liver phantom insert radius (mm)	29	16	8				
CR (no SC)	0.41	0.32	0.29				
CR (MC [1] SC)	0.88	0.60	0.69				
CR (CNN SC)	0.81	0.64	0.75				

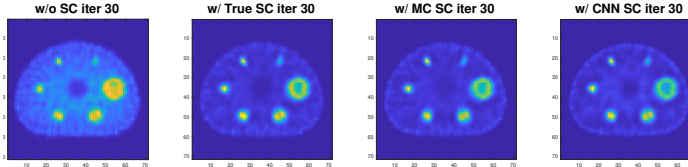


Fig. 3. NEMA-like phantom reconstruction at 30th iteration

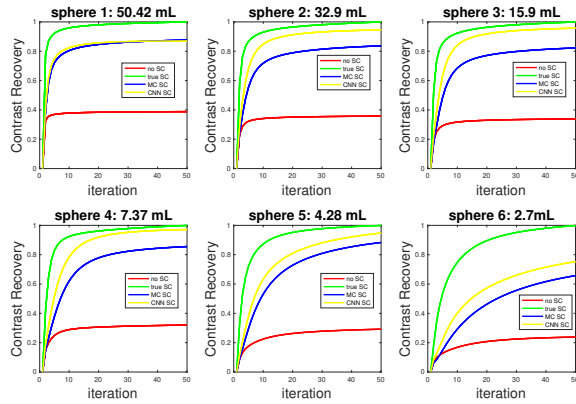


Fig. 4. NEMA-like phantom CR of 6 spheres over iterations

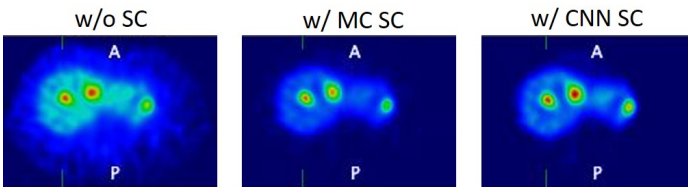


Fig. 5. Liver phantom measurement reconstruction at 30th iteration

IV. DISCUSSION

Compared with reconstruction without scatter correction, the proposed deep learning based scatter estimation method substantially improved contrast both in terms of visual image quality and CR in the Y-90 SPECT phantom studies. Furthermore, image quality and CR corresponding to the new scatter estimation method showed good agreement with results corresponding to our previous Monte Carlo based scatter estimation as well as results corresponding to ‘true’ scatter. These results are clinically relevant because once the CNN was trained, the scatter estimates were generated in a fraction of the

time it took to generate scatter estimates for the previous Monte Carlo based method (about 1 min for CNN vs. 1-2 hours for MC). The proposed method can be extended to SPECT scatter estimation applications other than Y-90 Bremsstrahlung SPECT by changing the training data. The training and test data in our study was limited and will be expanded in future studies. We will also include testing on clinical patient data. Furthermore, we will investigate training with 3D images instead of the projection space approach of the current study.

REFERENCES

- [1] Y. K. Dewaraja, S. Y. Chun, R. N. Srinivasa, R. K. Kaza, K. C. Cuneo, B. S. Majdalany, P. M. Novelli, M. Ljungberg, and J. A. Fessler, “Improved quantitative 90Y bremsstrahlung SPECT/CT reconstruction with Monte Carlo scatter modeling,” *Medical physics*, vol. 44, no. 12, pp. 6364–6376, 2017.
- [2] M. Elschot, M. G. Lam, M. A. van den Bosch, M. A. Viergever, and H. W. de Jong, “Quantitative Monte Carlo-based 90Y SPECT reconstruction,” *Journal of Nuclear Medicine*, vol. 54, no. 9, pp. 1557–1563, 2013.
- [3] Y. Berker, J. Maier, and M. Kachelrieß, “Deep scatter estimation in pet: Fast scatter correction using a convolutional neural network,” in *2018 IEEE Nuclear Science Symposium and Medical Imaging Conference Proceedings (NSS/MIC)*, pp. 1–5, IEEE, 2018.
- [4] H. Qian, X. Rui, and S. Ahn, “Deep learning models for pet scatter estimations,” in *2017 IEEE Nuclear Science Symposium and Medical Imaging Conference (NSS/MIC)*, pp. 1–5, IEEE, 2017.
- [5] J. Maier, E. Eulig, T. Vöth, M. Knaup, J. Kuntz, S. Sawall, and M. Kachelrieß, “Real-time scatter estimation for medical ct using the deep scatter estimation: Method and robustness analysis with respect to different anatomies, dose levels, tube voltages, and data truncation,” *Medical physics*, vol. 46, no. 1, pp. 238–249, 2019.
- [6] J. Bai, J. Hashimoto, K. Ogawa, T. Nakahara, T. Suzuki, and A. Kubo, “Scatter correction based on an artificial neural network for 99m tc and 123 i dual-isotope spect in myocardial and brain imaging,” *Annals of nuclear medicine*, vol. 21, no. 1, p. 25, 2007.
- [7] K. Ogawa and N. Nishizaki, “Accurate scatter compensation using neural networks in radionuclide imaging,” *IEEE transactions on nuclear science*, vol. 40, no. 4, pp. 1020–1025, 1993.
- [8] M. Ljungberg, S. Strand, and M. King, “The SIMIND Monte Carlo program,” *Monte Carlo calculation in nuclear medicine: Applications in diagnostic imaging*. Bristol: IOP Publishing, pp. 145–63, 1998.